COMPARISON OF TWO- AND THREE- DIMENSIONAL TRANSONIC TESTS MADE IN VARIOUS LARGE WIND TUNNELS

Xavier Vaucheret, et al

Foreign Technology Division
Wright-Patterson Air Force Base, Ohio

10 February 1976

FTD-ID(RS)I-0068-76

069144

FOREIGN TECHNOLOGY DIVISION

COMPARISON OF TWO- AND THREE-DIMENSIONAL TRANSONIC TESTS MADE IN VARIOUS LARGE WIND TUNNELS

by

Xavier Vaucheret, Maurice Bazin, and Claude Armand

Approved for public release; distribution unlimited.

42

UNCLASSIFIED

SECURITY CLASSIFICATION OF THIS PAGE (When Data Entered)

REPORT DOCUMENTATION PAGE		READ INSTRUCTIONS BEFORE COMPLETING FORM
1. REPORT NUMBER FTD-ID(RS)I-0068-76	2. GOVT ACCESSION NO	3. RECIPIENT'S CATALOG NUMBER
4. TITLE (and Subtitle) COMPARISON OF TWO- AND THREE- DIMENSIONAL TRANSONIC TESTS MADE IN VARIOUS LARGE WIND TUNNELS		5. TYPE OF REPORT & PERIOD COVERED Translation 6. PERFORMING ORG. REPORT NUMBER
7. AUTHOR(s) Xavier Vaucheret, Maurice Bazin, and Claude Armand		8. CONTRACT OR GRANT NUMBER(s)
9. PERFORMING ORGANIZATION NAME AND ADDRESS Foreign Technology Division Air Force Systems Command United States Air Force		10. PROGRAM ELEMENT, PROJECT, TASK AREA & WORK UNIT NUMBERS Dia Task Number PT-1850-10-75
11. CONTROLLING OFFICE NAME AND ADDRESS		12. REPORT DATE June 1975 13. NUMBER OF PAGES 42
14. MONITORING AGENCY NAME & ADDRESS(if different from Controlling Office)		15. SECURITY CLASS. (of this report) UNCLASSIFIED 15a. DECLASSIFICATION/DOWNGRADING SCHEDULE
16. DISTRIBUTION STATEMENT (of this Report) Approved for public release; distribution unlimited.		
17. DISTRIBUTION STATEMENT (of the abstract entered in Block 20, if different from Report)		
18. SUPPLEMENTARY NOTES		
19. KEY WORDS (Continue on reverse side if necessary and identify by block number)		
20. ABSTRACT (Continue on reverse side if necessary and identify by block number) 14		

DD FORM 1 JAN 73 1473 EDITION OF 1 NOV 65 IS OBSOLETE

UNCLASSIFIED

SECURITY CLASSIFICATION OF THIS PAGE (When Data Entered)

FTD- ID(FS)I-0068-76

EDITED TRANSLATION

FTD-ID(RS)I-0068-76 10 February 1976

FTD-76-C-000139

COMPARISON OF TWO- AND THREE-DIMENSIONAL TRANSONIC TESTS MADE IN VARIOUS LARGE WIND TUNNELS

By: Xavier Vaucheret, Maurice Bazin, and Claude Armand

English pages: 42

Source: Office National d'Etudes et de Recherches Aerospatiales, Number 1, 1975, pp. 1.1-1.14.

Country of origin: France
Requester: AEDC/DYF
~~Translator: Carol S. Hirsh~~
Approved for public release; distribution unlimited.

PREPARED BY:

TRANSLATION DIVISION
FOREIGN TECHNOLOGY DIVISION
WP-AFB, OHIO.

COMPARISON OF TWO- AND THREE-DIMENSIONAL TRANSONIC TESTS MADE IN VARIOUS LARGE WIND TUNNELS

Xavier Vaucheret, Maurice Bazin and Claude Armand

National Office of Aerospace Studies and Research (ONERA)
92320 Chatillon - France

Summary

In cooperation with several foreign research establishments, ONERA has undertaken a critical study of testing conditions at transonic speeds and of the validity of the data obtained in various Wind-Tunnels.

In two dimensional flow, two models of NACA 0012 and supercritical profiles have been tested in ONERA S3 Modane and RAE 15 x 60 inc. tunnels for a complementary field of Reynolds number, 4 to 40. 10^6 from Mach 0.3 to 0.9. Three homothetical profiles of NACA 0012 were also tested in S3 Modane. Wind tunnel wall interferences, including lateral boundary layer effects, are studied and recommendations on relative dimensions of models to test sections are made.

In three dimensional flow, four homothetical models of a typical transport aircraft were successively tested in twelve transonic tunnels commonly used for development tests in various countries. The data are compared in a broad range of Reynolds number (0.5 to 7 millions) between Mach number 0.7 and 0.96. The discrepancies obtained can be reduced with corrections due to the free tunnel and to the interference generated by the walls.

The effect of tripping the transition by grits is analyzed.

Lastly, comparisons obtained with an axisymetric body near Mach 1 are presented.

NOTATIONS

M	Mach number
P_0	Generator pressure
B	Width of test section
H	Height of test section
c	Local chord of one profile
$\bar{c}$	Mean chord of wing
S	Half-span of model
L	Length of model
R_c	Reynolds number based on c
$R_{\bar{c}}$	Reynolds number based on $\bar{c}$
R_L	Reynolds number based on L
P	Static pressure on wall
δ_1	Thickness of boundary layer displacement on lateral wall of wind tunnel
Q	Reduced porosity parameter (0 = closed test section, 1 = open test section)
α	Angle of attack of profile in two-dimensional flow
α_w	Angle of attack of wing chord
α_m	Angle of attack of model

COEFFICIENTS

C_D	Net drag (wind axis)
C_{Dp}	Drag obtained by integrating wall pressures in plane flow
C_{DW}	Wake drag in two-dimensional flow
C_{Df}	Skin friction drag
C_L	Lift (wind axis)
C_A	Drag (model axis): axial force
C_N	Lift (model axis): normal force
C_m	Pitching moment (at 25% of c, or $\bar{c}$)
$C_{N\alpha^o}$	Lift gradient ($C_{L\alpha^o}$)
$\bar{x}/\bar{c}$	Position of neutral point

C_p Pressure coefficient

v/U Coefficient of lateral suction in plane flow

SUBSCRIPTS

c Denotes value at C_N zero

u Denotes uncorrected value

c Denotes corrected value

i Denotes value resulting from integration of pressures on profile

1. TWO-DIMENSIONAL TESTS

1.1. Objectives of Study in Plane Flow

Considerable work has been done in the area of tests in plane flow with the development of new generations of profiles for more high-performance aircraft or helicopters. These tests form the experimental basis for developing theoretical methods of designing profiles.

Parallel to constructing and developing a two-dimensional test section in the S3 Modane Avrieux wind tunnel [1], a program designed to qualify the equipment and testing techniques in the transonic region was set up by ONERA in conjunction with the official French services. Three homothetic models of the NACA 0012 profile were made for an experimental study of wall effects.

- The chord C = 0.15 m (C/H = 0.19) corresponds to the smallest compatible size with the minimum distortion when loaded, an adequate number of intakes and the potential for obtaining the same Reynolds number in the S3 MA as with the largest model.
- The intermediate chord is C = 0.21 m (C/H = 0.27).
- The longest chord C = 0.3 m (C/H = 0.38) is purposely oversized with respect to the test section in order to determine the validity limits for the wall effect corrections.

The conventional blockage of the test section by these three models is very important, being compared to the usual values during three-dimensional tests in the transonic region: 2.3%, 3.2%, 4.6%.

A collaboration with the National Aeronautical Establishment in Ottawa made it possible to test the NACA 0012 model with an 0.3 m chord in the 15×[illegible] inch wind tunnel [2], in which a ratio of $c/h = 0.197$, which is close to that of the model with a 0.15 chord in the S3 MA, was then obtained. Like the S3 MA, the NAE wind tunnel made it possible to test this profile from M = 0.2 to M = 0.9, supplementing the range of Reynolds numbers which went from 4 to 14.10^6 at Modane up to 40.10^6.

The physical difficulties of adapting a two-dimensional model to different wind tunnels explains the limited extent of these comparisons among several wind tunnels. Differences in test section width, attachment and pneumatic couplings make it necessary to either make major changes in the model or a design of complex origin, thus one which is costly. This was the case for the model of the LC 100 D supercritical profile with a 0.3 m chord recently tested in the two previous wind tunnels.

The results of testing various models of the NACA 0012 profile were exchanged between several wind tunnels, eg., the ONERA and the N.P.L. The experimental conditions and different test programs make it difficult to make direct comparisons.

The determination of the aerodynamic coefficients by integrating numerous wall pressures and by combing the wake imposes limitations on the angle of attack, whose extent limits the number of points defining one polar in intermittent wind tunnels. In these conditions, the interpolations are not precise enough to permit the direct comparison of several tests made under identical conditions before and after correction for wall effects or in several wind tunnels. This is all the more true because wall effects are great in two-dimensional flow.

The model used in the NAE wind tunnel was very light-weight. It is certainly necessary to avoid stray circulation or friction at the ends of the model and to obtain a flow which is strictly two-dimensional along the span, including on the periphery of the two walls.

Without presenting the different methods of making wall effect corrections during this discussion, it is appropriate to remember that one of the major difficulties is defining the coefficient of aerodynamic permeability of perforated walls due to the large number of parameters affected. With homothetic models, the variation in generator pressure needed to obtain results at the same Reynolds number on the models modifies the behavior of permeable walls.

In the S3 MA, the reference formed by the closed test section was used as frequently as possible due to the small corrections in angle of attack obtained in this particular case and the theoretical knowledge of the coefficients to be used.

The coefficients used in the NAE were provided from past experiments and pressure measurements taken on the walls of the wind tunnel.

Generally speaking, the coefficient which defines wall permeability is determined by matching the lift gradients to those obtained in the closed section after correction (Fig. 1).

The linearized theory of compressible fluids, bringing the integrated coefficients into play, does not allow one to obtain corrected results of the effects of uniform walls between the model with the 0.3 m chord and the two other models in the S3 MA. The method developed by Mokry at NAE [3], which brings a series for translating the experimental distribution of pressures on the model into play, compares the results. A new method, which was also developed at NAE, uses pressure measurements taken on the test

section walls to determine the permeability coefficient to be used [4]. This method is undergoing development at ONERA.

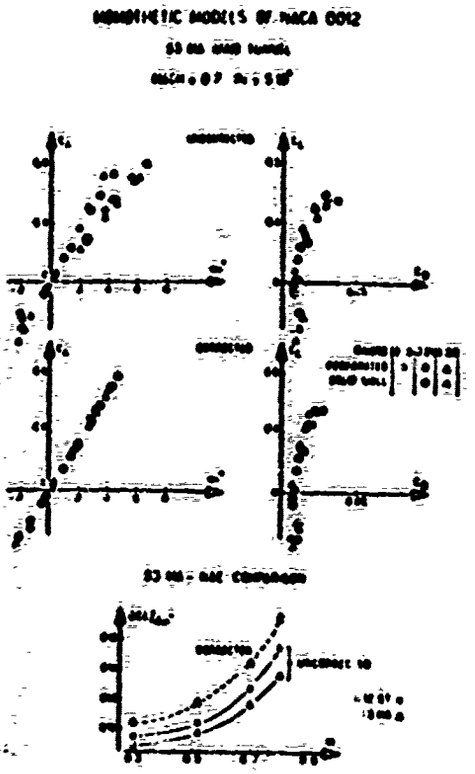

1.2. Effect of Lateral Walls

In a plane flow, the walls located above and beneath the model are the source of the usual interference to which various correction methods are applied.

The boundary layers which develop on the lateral walls of the wind tunnel alter the two-dimensionality of the flow and constitute a parasitic effect which should be minimized.

For the S3 MA, this result was obtained by using a very large test section, B/H = 0.72, which was a compromise between parameters

such as: the model's rigidity, the quality of the shadow photography, the flow of air in the wind tunnel and correct two-dimensionality, which does not alter the pressure measurements on the axis of the wind tunnel. The calculations and, most of all, visualizations indicated [1] satisfactory flow most of the time with limited breakaway on the profile.

At NAE, B/H = 0.25, suction of the lateral boundary layers and the model was aimed at obtaining the desired result in a test section which was relatively narrower.

In our opinion, the qualification of lateral suction and its effect on breakaway remains a delicate problem, as several tests made during the ONERA-NAE collaboration indicated. It is often difficult to account for the parameter of lateral suction in wind tunnel comparisons.

Several qualifying criteria for lateral suction can be used: the track of the rectilinear and parallel shock on the leading edge, the wall flow parallel to the walls shown by oil visualizations. The distribution of wake drag C_{D_W} must be uniform across the span. A comb with four probes was used at NAE.

The two situations shown in the upper part of Fig. 2 satisfy these three criteria more or less simultaneously. In one case, the shock is rectilinear, the flow is directed well on the test section axis where the wall pressure measurements were taken and the wake drag is constant along the span. In the other case, the shock curves inward, but the flow is parallel to the walls at the corners of the trailing edge. Wake drag develops with the span, which would seem to exclude too high a suction ratio for this moderate angle of attack. A raised suction ratio is necessary at large angles of attack in order to avoid premature stalling at the walls.

These two practical rules for lateral suction correspond to very different wall pressure distributions with respect to the

position of the shock and the breakeway behind it. Similar effects were found with the LC 100 D supercritical profile.

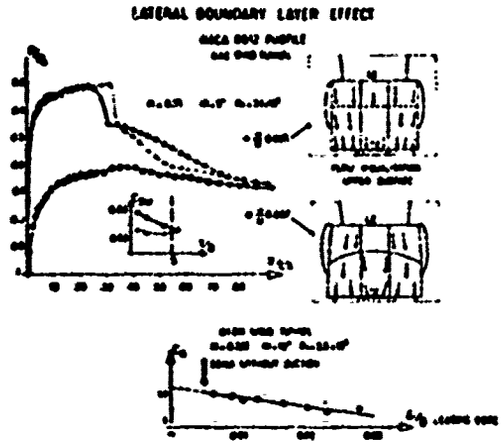

Systematic tests of the suction of lateral boundary layers have currently been developed in the ONERA R1Ch wind tunnel (B/H = =0.21). The lower part of Fig. 2 shows some of the first results of these these tests, here at a low Mach number. The lateral suction control in front of the model makes it possible to vary the depth of the movement of the boundary layer, which is measured to the right of the leading edge of the model. A variation of 10% of the coefficient of normal force CN is observed between the flow without suction and the value obtained when assuming the boundary layer to be completely elimated. This result justifies the technological complexity of a boundary layer suction device. The value obtained without suction in the S3 MA is plotted on the curve.

1.3. Determining Drag

It is possible to obtain drag, excluding friction, by integrating wall pressures. The total drag is calculated from the

pressures in the wake for the S3 MA as well as NAE. Weight is used as a cross-check in the NAE equipment.

Figure 3 shows an interesting feature of drag determined by combing the wake. This coefficient is not greatly affected by wall effects. The same results are obtained in the NAE and S3 MA in the closed test section and the permeable test section. They confirm the theoretical predictions.

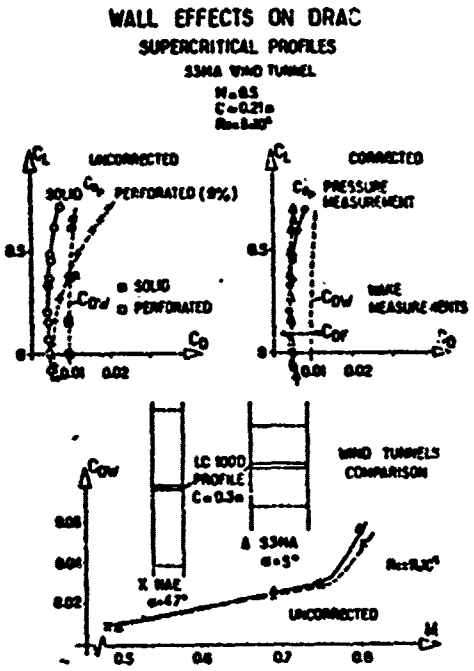

Thus, although measuring drag by combing the wake is a delicate procedure, it is fundamental.

The comparison of pressure drag for two different walls of the S3 MA wind tunnel shown in Fig. 3 shows the value of tests in closed test sections for determining this coefficient, which is hardly affected by the solid wall.

The uncorrected results from a permeable test section make a pseudo "elongation effect" appear which is incompatible with the two-dimensional tests and can surprise the experimenter with a total drag which is less than the pressure drag.

Everything falls into place after correction, except at a large angle of attack, where a slight breakaway effect which has not currently been controlled exists.

1.4. Effect of Reynolds Number

The interesting potentials of the NAE wind tunnel made it possible to supplement the tests made in the S3 MA up to R_c = = $14 \cdot 10^6$ through $R_c = 40 \cdot 10^6$ [5].

Figure 4 gives two examples with the three homothetic models of the NACA 0012 profile for S3 MA and the tests in a permeable test section at Mach 0.7, used elsewhere to characterize the development of the permeability coefficient with generator pressure.

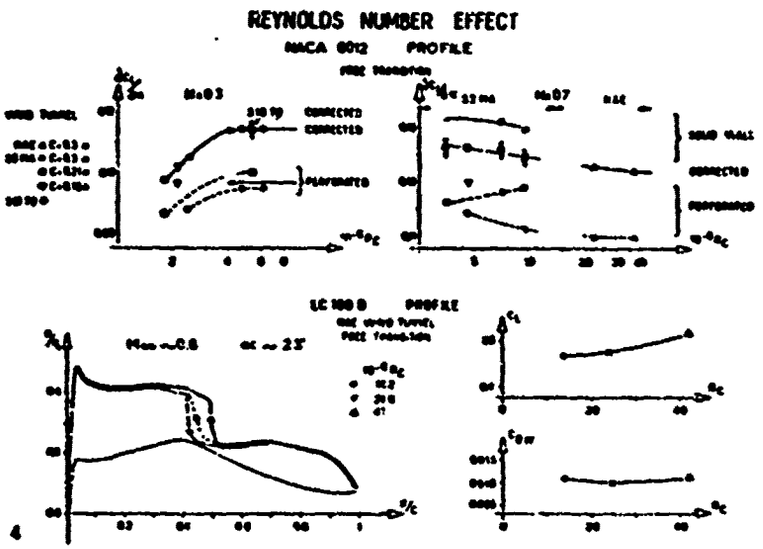

At M = 0.3 the results (up to $R_c = 26 \cdot 10^6$ at NAE) show that the effect of the Reynolds number on $\partial C_Y / \partial d$ becomes negligeable beyond $5 \cdot 10^6$. The point obtained on the same profile in the closed test section in the S10 wind tunnel of Toulouse (C/H = 0.34 - B/H = 0.45 - C = 0.75 m) is shown.

At M = 0.7 it is necessary to reach $R_c = 30 \cdot 10^6$ in order to see the effect of the Reynolds number disappear. This appears to be reversed in the S3 MA on the profile with a chord of 0.21 m due to the wall effects.

At M = 0.8 the shock recoils up to $R_c = 41 \cdot 10^6$ on the LC 100 D supercritical profile (Fig. 4). Considering the sensitivity of the position of the shock to the effects of the Mach number and the conditions of lateral suction, it is always necessary to be very careful when interpreting this result.

1.5. Recommendations

The experience acquired during these different tests makes it possible to state two aspects of the effects of walls in a plane current.

. The chord of the models must not be greater than C/H = 0.25 in the case of currents. This value is the result of a compromise between the wall effects and technological reasons such as: distortion and equipment for taking pressure readings upon which the precision of the measurements depends.

Unfortunately, one can end up with a value of C/H = 0.35 when using specific equipment for studying focal flows (a boundary layer scanner, unstationary pressure pick-ups, hot skins such as those for the LC 100 D profile) or for displaying the nose or flaps and their supports realistically.

. The parametric study of wall effects based on the linearized theory of compressible fluids (Fig. 5) is confirmed by the preceding experiments. The practical example in Fig. 5 is an extreme case because of the Mach range in question as well as the choice of aerodynamic coefficients. It was designed to show the relative effect of the different corrections in two-dimensional flow. It seems that the closed test section limits the interference of the angle of attack and drag considerably.

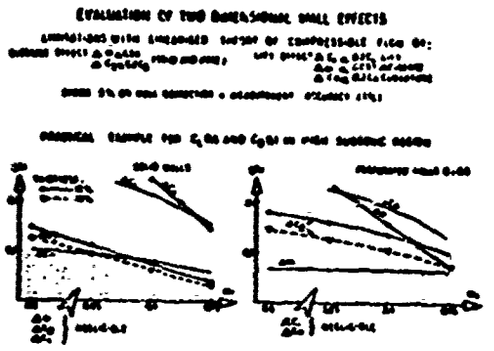

However, the use of a test section with permeable walls makes it possible to limit the effects of blockage at high Mach numbers and, most of all, the curvature of field ΔC_m, which directly affects pressure distributions and the position of the shock and whose correction is not readily accessible, no matter what the Mach number.

Still, this type of test section requires research on the permeability coefficient by means of several tests in a closed test section (easily achieved by gluing a plastic covering over the wall perforations).

Since we are trying to discover the distributions of experimental pressures rather than overall coefficients, it is preferable to use permeable walls and accept a correction for reference angle of attack and drag which is less precise.

2. THREE-DIMENSIONAL TESTS

2.1. Objectives of Study of Aircraft Models

Discrepancies are usually noted when comparing the results obtained for aircraft models in different wind tunnels. In the transonic region, in particular, the difference in the types of ventilated walls used results in different wall interferences which become intensified as the Mach number increases. In 1952 and 1954, two three-dimensional calibration models were selected by AGARD to compare transonic and supersonic wind tunnels; these models, called AGARD B and C, consist of a delta wing with a thin profile with a thickness of 4% mounted on large rotating bodies. The conclusions stated in 1961 [6] indicated that these models were well adapted to the supersonic, but must be replaced by a configuration which was closer to that of a typical aircraft in order to make a valid comparison in the transonic. This is why ONERA proposed to determine calibration models suitable for the transonic mode in 1970 to the French official departments and designers. The choice was made in favor of representative models of a typical transport aircraft [7], called ONERA calibration models, thus bringing to light the problems related to the transonic region, including the effect of blockage by models and the sensitivity of the Reynolds number.

A set of homothetic models proved to be necessary in order to satisfy two objectives: first of all, to make comparisons of wind tunnels with different dimensions in the best conditions, i.e., with similar blockage. Then, for the purpose of an experimental approach to wall interference, to study the effect of blockage in the same wind tunnel. The definition of two blockage limits was planned: the lower limit, below which wall effects can be considered to be negligeable and thus can be used as references for tests on larger models; and the upper limit, beyond which the wall corrections of the linearized theory are no longer valid.

A set of four homothetic models was completed in 1972. The first results, published in April of 1972 as the offshoot of the LAWS group [8], involved four wind tunnels: the S2 and S3 Modane, the Σ4 of the St. Cyr Institute and the 1 m^2 wind tunnel of the

DFVLR at Göttingen. Twelve wind tunnel-model pairs were compared. After making tests on the models in three other transonic wind tunnels - the S4, HT and TVM of the FFA at Stockholm - a comparison of 20 model-wind tunnel pairs was presented to the EUROMECH 40 Congress in 1973 by the FFA [9]. After tests in the S3 Chalais wind tunnel of ONERA, the models were sent on in 1974 to wind tunnels 11 T of NASA Ames, 4 T and 16 T of the AEDC at Tullahoma and 5 T of the NAE at Ottawa. At this time, the comparison dealt with 31 model-wind tunnel pairs obtained in 12 European or American wind tunnels. This is the most extensive comparison of methods for taking measurements using aircraft models that has been made since the creation of transonic wind tunnels. It should be noted that the largest of the four calibration models, with a span of 1 meter and equipped with pressure valves, was tested in five wind tunnels with a test section cross section exceeding 1.5 m^2 currently being used for industrial tests of aircraft designs.

At the same time, in cooperation with other departments, the AEDC undertook [10] an international comparison of the qualities of transonic flows in wind tunnels using a calibration cone with an opening of 10 degrees for the purpose of measuring boundary layer transitions and noise levels.

2.2. Models

The shape of the calibration models (Fig. 6) is representative of a transport aircraft in the Mach 0.85 class (the drag divergence Mach number is 0.866).

A wing, a horizontal empennage and a fin with leading edge sweeps of 30^o, 37^o5 and 47^o5, respectively, are mounted on a rotating fuselage with little constraint on the base for installation of the right sting. The wing aspect ratio is 7.3. The same "Peaky" symmetrical profile with a relative thickness of 10.5%, developed at ONERA, is used to outfit all the lifting surfaces.

Set on the fuselage at a 4° angle, the wing has no twist. The lack of twist and curve in these swept wings with a high aspect ratio results in characteristics of premature stall at the tip of the wing, allowing an interesting comparison of the "pitch-up" thresholds obtained as a function of M and Re in various wind tunnels.

The geometry of the models was simplified as much as possible to ensure high precision of construction: all the lifting surfaces have conic generation and there are no "pocket" fillets. The permissible error in construction was set at 3/100 mm. The homothetic shape of the sting supports was observed over a length equal to 6 diameters of the base behind the base. One particular test made in the S3 Modane wind tunnel (Fig. 7) shows that a 50% enlargement of the sting shapes behind the zone in which homotheity is observed only affects the ascent of the test section (curves CN and α are parallel) and slightly affects the pitching moment between "pitch-up" and "pitch-down."

The ensemble of the 4 models M1, M2, M3 and M5 in scale ratios of 1, 1.28, 1.65 and 3.42 result in a span range from 0.3 to 1 meter. The largest model, M5, has pressure valves on 3 chords of the wing at a rate of 40 intakes per chord. The pressures are measured by 3 scan valves lodged in the nose of the fuselage, making it possible to rapidly and simultaneously take down information on measurements of internal balance forces with 6 components.

Four "equivalent" rotating bodies with the same cross-section laws as the aircraft models were also made. Rotating body C5, which corresponds to model M5, has pressure valves on 2 generatrixes (85 intakes in all) for making special studies in the Mach 1 range.

2.3. Wind Tunnels

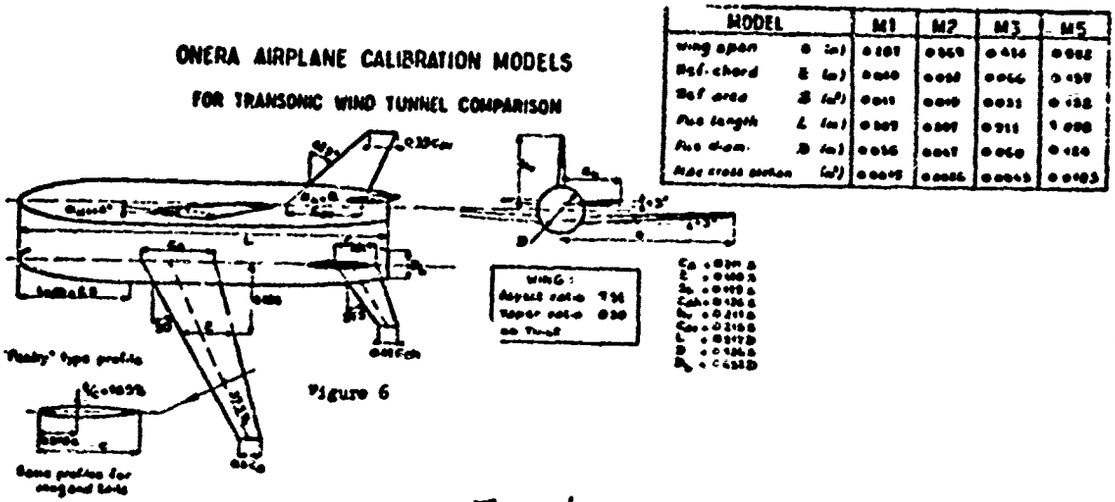

Fig. 6.

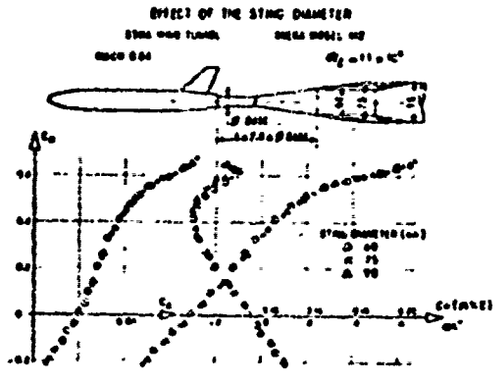

Fig. 7.

The 12 wind tunnels compared (Fig. 8) were grouped into four classes according to the nature and number of ventilated walls:

- 4 perforated walls:
  AEDC/16T and 4T - NAE/5T - S3 MA - AVA/1m - FFA/TVM
- 2 perforated walls:
  S2 MA - S3 Ch - Σ4/St. Cyr
- 4 slotted walls:
  NASA Ames/11T - FFA/HT
- 2 slotted walls:
  FFA/S4

Tests were made on the two wind tunnels with adjustable permeability - AEDC 4T and S2 MA - with different wall porosities.

The table in Fig. 8 shows the obstruction values (blockage in %) and the test section span/width ratio values (2S/B). The six cases for which the wall corrections are negligeable are outlined with heavier marks. Obstruction must be less than 0.1% and

the span, less than a fifth of the test section width, to satisfy these conditions. On the other hand, the obstructions are close to 1% and the span/width ratios of the test section exceed 0.7 in the two extreme situations, M3 of the S3 MA and M2 of the FFA/TVM.

ONERA AIRPLANE CALIBRATION MODELS

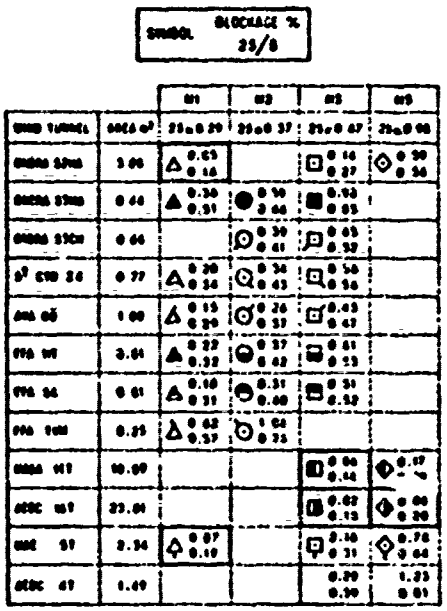

NOTE: The incomplete results of the AEDC 4T wind tunnel are not given hereafter. The symbols in the table (Fig. 8) are those used in Figures 11-15 and 18-20.

2.4. Test Program

The "comparative" test program involves variations in angle of attack at Mach numbers from 0.7 to 0.96 with a Mach interval of 0.02 beyond Mach 0.84. Several generator pressures were realized at Mach 0.84 for the wind tunnels with variable density, i.e., in the transonic "cruising" mode, before the divergence in drag for moderate C_N.

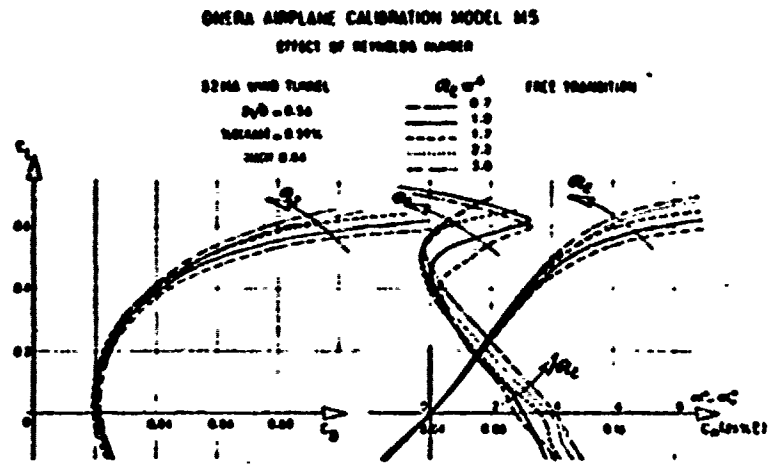
ONERA AIRPLANE CALIBRATION MODEL M5
EFFECT OF REYNOLDS NUMBER
FREE TRANSITION

FIG. 9.

The tests were made in the natural transition except for in the NASA and AEDC wind tunnels: here boundary layer transition was triggered by 0.6 mm glass beads glued onto the nose of the model and at 8% of the depth of the chords on the upper and lower wing surfaces of all the lifting surfaces. However, for the sake of comparison NASA and AEDC made variations in the Reynolds number at Mach 0.84 in the natural transition.

The Reynolds number calculated on the mean chord for the group of wind tunnels at Mach 0.84 varied from 0.2 to 7.2 million. The classic curves - polar, CL (α), CL (C_m) - obtained in the natural transition (Fig. 9) bring out the models' sensitivity to the Reynolds number: as the Reynolds number increases, lift increases, induced drag and minimum drag decrease and the "pitch-up" and "pitch-down" zones are displaced toward great lift. At low lift the irregularities in the pitching moment are absorbed: the stability curves become linear and the pitching moment at zero lift increases with the Reynolds number.

2.5. Results

2.5.1. Generalizations

Each cooperating organization furnished rough results, i.e., uncorrected results, of wall effects. These results were processed by ONERA in a strictly uniform manner using a calculation program which interpolated the results to round CN values by means of sliding curves which passed through 4 consecutive points. On the basis of the interpolated values, the derivatives leading to the lift gradients and the positions of the neutral points are found by finite differences with a unique CN interval of 0.2.

Because of variations in the Mach number recorded in certain wind tunnels during variations in angle of attack as well as variations in the Reynolds number from one wind tunnel to another, the curves are presented at a constant CN, either for the

Mach number of 0.84 as a function of the Reynolds number, or as a function of the Mach number for very close Reynolds numbers.

In any case, the classic curves obtained at Mach 0.84 in three wind tunnels on the same model, M5, are presented (Fig. 10) at two Reynolds numbers as an example: 1.02 and 2.22 million. The results are standerdized to their values at zero lift. The agreement of the polar and CL (α-α_0) curves is excellent. On the other hand, the stability curves differ all the more because the lift and the Reynolds number are raised without affecting the "pitch-up" threshold. The spread of the curves follows the increase of the span relative to the width of the test tunnel well. The maximum deviation between the results for longitudinal stability corresponds to a 5% variation in the position of the neutral point.

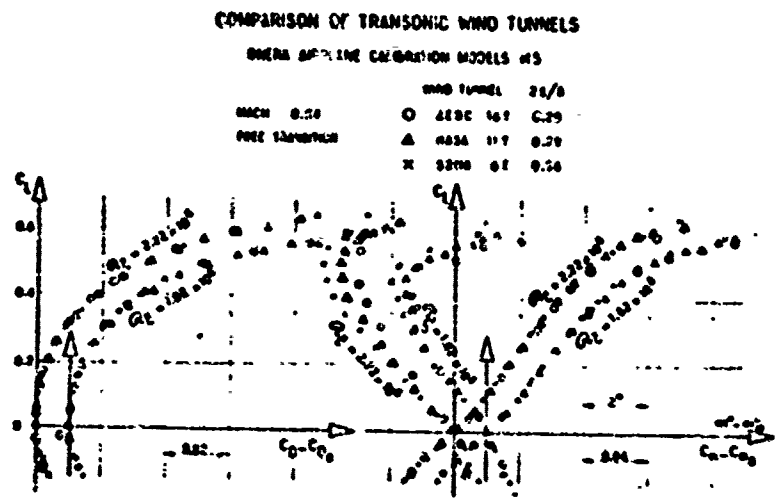

FIG. 10.

2.5.2. Developments Accompanying the Reynolds Number at Mach 0.84

The developments of different model curves with the Reynolds number at Mach 0.84 in the natural transition are presented in Figures 11 to 15: drag, pitching moment, lift gradient,

FIG. 11.

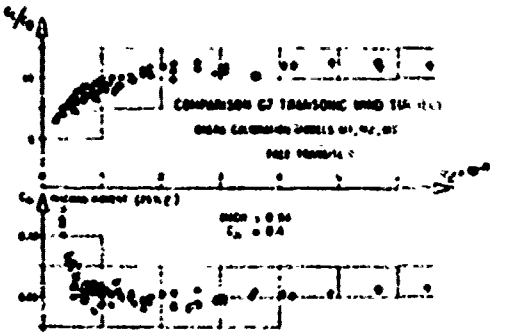

FIG. 13.

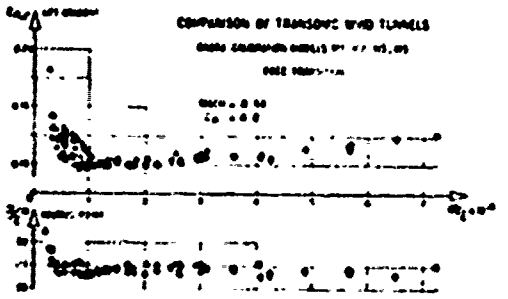

FIG. 12.

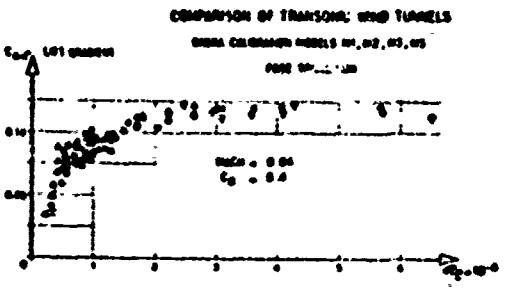

FIG. 14.

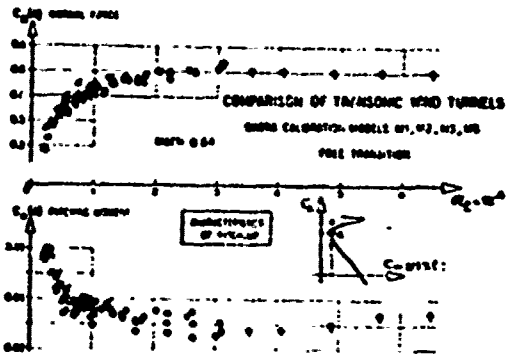

FIG. 15.

position of neutral point at zero lift (focus); lift-drag ratio, pitching moment, lift gradient at CN = 0.4; and the values of the lift and pitching moment coefficients which define entrance into "pitch-up." The following remarks can be isolated from this set of developments:

- The dispersion of points appears small at the limiting Reynolds number values because there are few results: only three wind tunnels (FFA, HT, AVA and AEDC 16 T) below $R_c = 0.4 \cdot 10^6$ and only one wind tunnel (NAE, 5 T) above $3.7 \cdot 10^6$. On the other hand, there appears to be a great dispersion of points around $1 \cdot 10^6$ because the largest number of points in the comparison are here (16 model-wind tunnel pairs). Thus, one cannot conclude that the dispersion varies with the Reynolds number.

- The developments accompanying the Reynolds number are very rapid below $1 \cdot 10^6$. On one hand, they confirm the extreme difficulty of comparing results which are not obtained at precisely the same Reynolds number and on the other, the difficulty of making predictions based on tests at very low Reynolds numbers.

- There is no rapid development with the Reynolds number above $3 \cdot 10^6$.

- None of the results referring to a model or wind tunnel deviate notably from the cluster of points, whether dealing with the smallest or the largest model. Thus, it is not permissible to suspect that the homothetity of the models is imperfect or to conclude that one test section is of higher quality, whether it has perforated or slotted walls on all four sides or only on the bottom/top.

- The results are more scattered at a lift of $C_N = 0.4$ than at zero lift due to the presence of breakaway. In any case, the "pitch-up" curves (Fig. 15) are not very scattered considering the difficulty of determining them, the lift curve in particular (point of $\frac{\partial C_m}{\partial C_N} = 0$ given by the interpolation program).

- The curve of drag at zero lift (Fig. 11) exhibits the classic decrease in the laminar regime as the Reynolds number increases. The transition zone between the laminar and turbulent

areas, where drag increases with the Reynolds number, can only be discerned on the curves corresponding to a given wind tunnel and model. This transition zone is located between 2 and 3 million. Thus, it appears desirable to make tests at Reynolds numbers exceeding 3 million in order to avoid the rapid variations caused by flow which is too laminar.

Local pressure measurements made on the largest calibration model M5 also bring out the interest in tests made at Reynolds numbers which are based on the outer chord of the wing this time, exceeding 3 million. According to the results from 4 wind tunnels, the pressure distributions (Fig. 16) on the outer chord of a wing located at 81% of the span show that as the Reynolds number increases, the shock recoils up to 3 million, then advances moderately beyond this. At the same time, the decrease in the depression on the trailing edge indicates the progressive reabsorption of breakaway. The lift coefficient obtained by integrating the pressures increases notably up to a local Reynolds number of 3 million, then decreases beyond this.

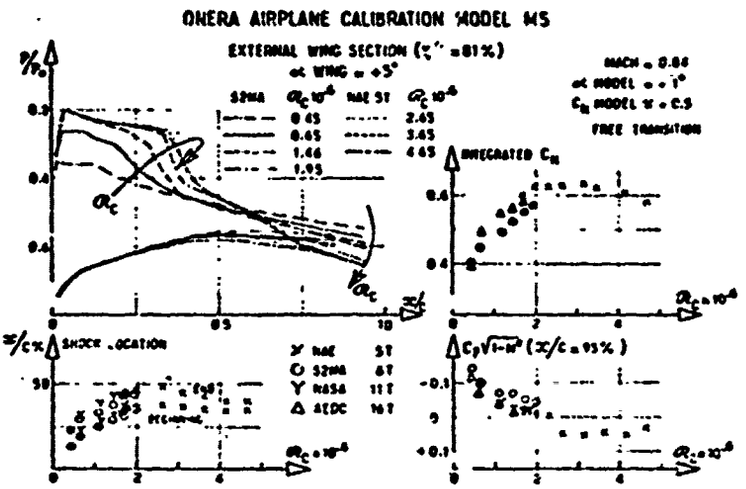

FIG. 16.

The lift coefficients integrated on the three chords of model M5 (Fig. 17) and the pressure coefficients of the trailing edge plotted as a function of the angle of attack for four Reynolds numbers (corresponding to the four test generator pressures) on the basis of tests made in two wind tunnels (the NASA Ames 11 T and the AEDC 16 T) are identical. The curves are a good illustration of both the propagation of breakaway along the span from the wing tip and its reabsorption with the increase in the Reynolds number. The pressure of the trailing edge reveals the appearance of breakaway which accompanies loss of lift. As the angle of attack increases, breakaway causes it to become even greater - 1 degree on the cross section of the wing tip and 1.5 degrees on the central cross section - while it is not visible on the wing root cross section at the lowest Reynolds number. When the Reynolds number is increased 4 times, the angle of attack at which breakaway appears increases by 1 degree. At a Reynolds number of 1 million, stalling which occurs at an angle of attack of from 1 to 2 degrees on the wing tip only occurs between 2.5 and 4 degrees on the central section and it is not experienced at all at the root.

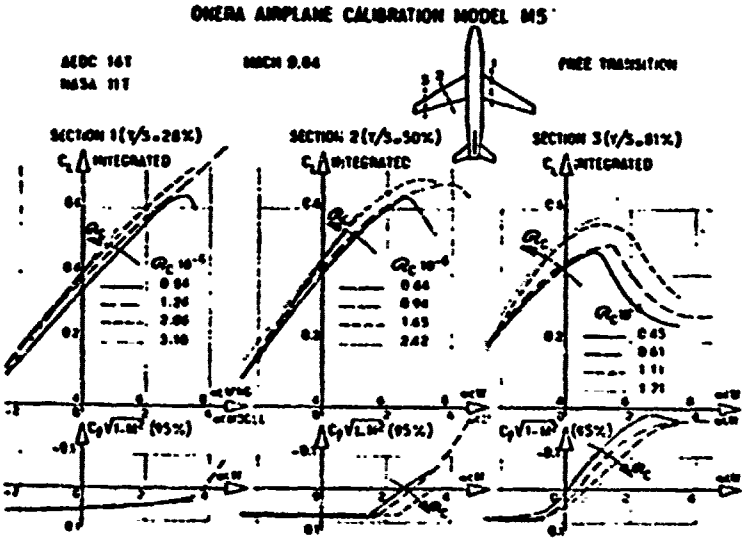

FIG. 17.

2.5.3. Development Accompanying Mach Number at $R_{\bar{c}} = 1 \cdot 10^6$

The comparison of the variations in model curves with the Mach number can encompass the most points at a Reynolds number of 1 million. Considering the still marked development of the curves around this low Reynolds numbers, only the results contained in the narrow plateau from 0.9 to 1.1 million were retained. The results (Figures 18 and 19) lead to conclusions similar to those in the preceding paragraph, i.e., that none of the blockage values or wind tunnels can symptomatically be freed from the cluster of points.

As the Mach number increases, the discrepancies at zero lift increase with respect to the lift gradient or focus as much as to drag. On the other hand, the scattering of precise results measured at $C_{II} = 0.4$ decreases due to the linearization of the curves (C_{II}, α) beyond Mach 0.9 for the type of model in question.

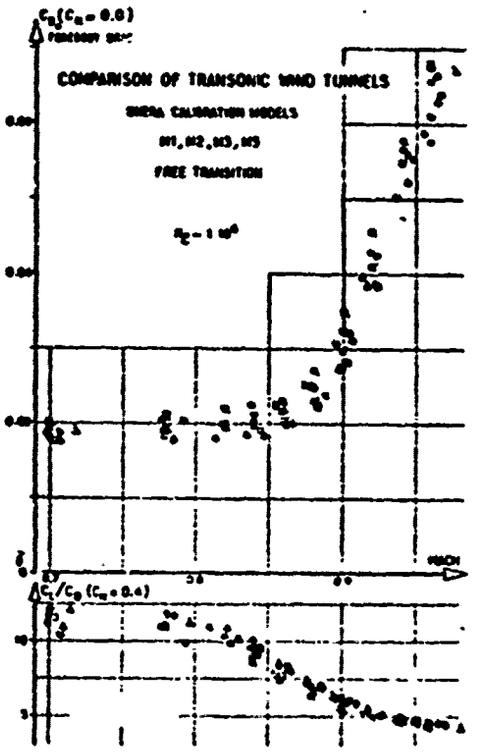

FIG. 18.

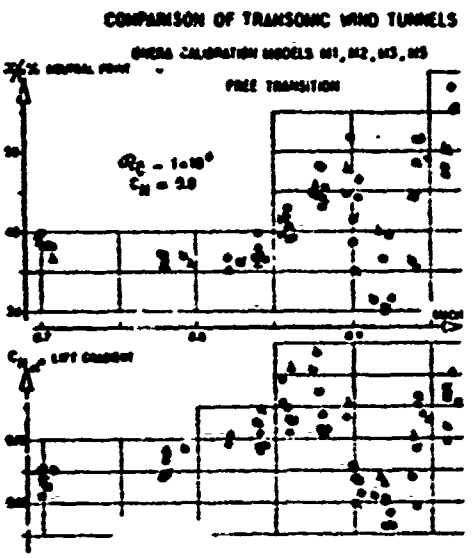

Fig. 19.

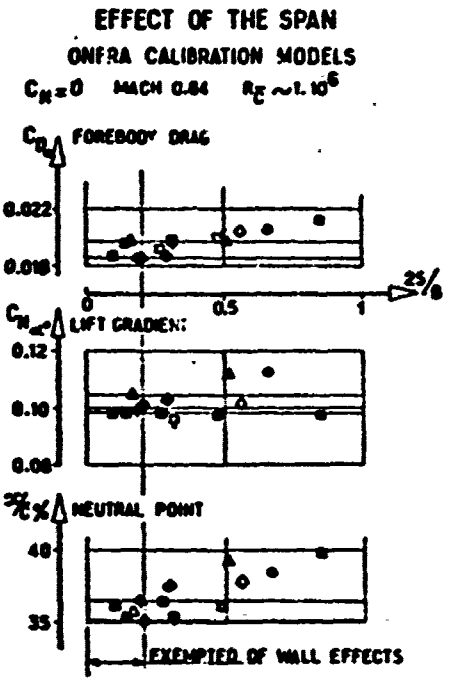

Fig. 20.

2.5.4. Comparisons at Mach 0.84, $R_c = 1.10^6$

Keeping only the results included in the plateaus of the Reynolds numbers (0.9 to 1.1 million) and Mach numbers (0.838 to 0.842) in order to be free of the developments accompanying these two parameters, twelve results can be retained. The total deviations between the results are as follows:

C_N	0,0	0,4
ΔC_D	0,0035	0,0074
ΔC_m	0,022	0,018
ΔC_{N_α}	0,017	0,025
$\Delta x/c$ %	4,7	10,9
$\Delta C_L/C_D$	-	1,48

Stating the results as a function of the span/width ratio of the test section (Fig. 20), it is very clear that at small values of this ratio, lower than 0.2, i.e., those at which the wall corrections are negligeable, the deviations are clearly reduced. The following table shows this reduction in deviations:

C_N	0,0	0,[illegible]
ΔC_D	0,0013	0,0031
ΔC_m	0,021	0,006
$\Delta C_{M_{\alpha^2}}$	0,006	0,010
$\Delta x/c$ %	1,2	5,2
$\Delta C_L/C_D$	-	0,93

The deviations obtained represent approximately 25% of those taken for all the results, except for the pitching moment at zero lift, which remained virtually unchanged. Thus, one might hope that the application of corrections for wall effects would considerably reduce the discrepancies between the compared values.

2.6. Corrections to be Applied

The results given above were rough, i.e., uncorrected. It is necessary to distinguish the corrections for the wind tunnels, no matter what the size of the models, from those connected with wall effects. The first category includes:

- the corrections for the longitudinal static pressure gradient, empty test section; the correction for static reference pressure and the correction for drag (buoyancy). These corrections can be nullified by adjusting wall divergence and the position of the reference pressure valve. But these adjustments vary as a function of the Mach number and the test generator pressure. Also, it is impossible or undesirable to change divergence during

tests in many wind tunnels. Moreover, wall divergence accounts for the development of the boundary layers on the walls, but not the change in these boundary layers when models are present;

- the corrections for the ascent of the empty test section, which are defined from classic tests with a model placed in the normal, then inverse position in succession;

- the corrections for the field of the sting supports, in particular when they are placed at an angle. In this report, special precautions were taken to observe the homothetity of the shapes behind the base of the models;

- the corrections for the level of flow fluctuations in the test section, both for pressure (noise) as well as for velocity (turbulence). The effect of these fluctuations is an area which has not been explored enough to try to make such corrections. However, their importance must not be underestimated, for they affect the transition positions of the boundary layers as well as the appearance and intensity of the phenomena of breakaway. Very different vibrational behavior was revealed during comparisons of different wind tunnels with the same model or different models in the same wind tunnel. Thus, it was possible to carry out tests in the S2 Modane wind tunnel on the smallest model (M1) up to beyond the "pitch-up" point without major vibrations, while tests on the largest model (M5) had to be discontinued soon after "pitch-up" in order to avoid damaging the scales measuring the forces. This variation in behavior can be due to frequencies in the assembly itself or to flow fluctuation levels.

The so-called wall corrections [11, 12] include:

- the corrections for volume and wake blockage, involving corrections in static reference pressure in interaction with the field of the model; corrections in the Mach number and dynamic pressure, thus all the aerodynamic coefficients; and corrections

for drag caused by the longitudinal velocity gradients of the interference induced by the wake and volume of the model. The last element is the most important correction in the transonic regime;

- the so-called lift corrections, which modify drag and angle of attack in the overall sense and the curvature of the field to the right of the wing and the empennage, thus the pitching moment, in the local sense.

The diverse wall corrections essentially depend on the parameter of aerodynamic porosity of the walls. The means of obtaining this parameter will be explained in a report to be presented at the AGARD/FDP Symposium at London in October of 1975 [13].

The following three references can be considered in order to obtain the aerodynamic porosity values as a function of the Mach and Reynolds numbers:

- tests on the same model in the same closed test section (all pores are blocked)
- tests on the same model in a wind tunnel which is clearly larger
- tests on a homothetic model which is much smaller in the same wind tunnel with permeable walls.

These three methods were successively applied to the results obtained on ONERA calibration models in the S2 Modane wind tunnel. Only the last one is presented here. The results obtained at the same Reynolds number (0.7 million) as a function of the Mach number on the two homothetic models M1 and M5 in the S2 Modane wind tunnel are shown here before and after correction in Figures 21 and 22. After the "wind tunnel" corrections were applied to the results from the smallest model (M1), for which the wall corrections are negligeable, the porosity parameter was adjusted so that the set

of results from model M5 agree as much as possible with those from model M1, serving as the reference model. After all the corrections, the results agreed satisfactorily: the deviations between the corrected results for the two models are on the order of one fifth those before the corrections and are compatible with the scattering of measurement. It should be noted that this agreement could only be obtained after applying the wind tunnel corrections based on the very careful calibration of the empty test section. The portion of this correction in the drag coefficients (Fig. 21) is 5% and 1%, respectively, in the raised subsonic for models M1 and M5. This correction exceeds the wall corrections between Mach 0.7 and 0.85. On the other hand, above Mach 0.85 the wall corrections become larger and larger, reaching 12% of their corrected value.

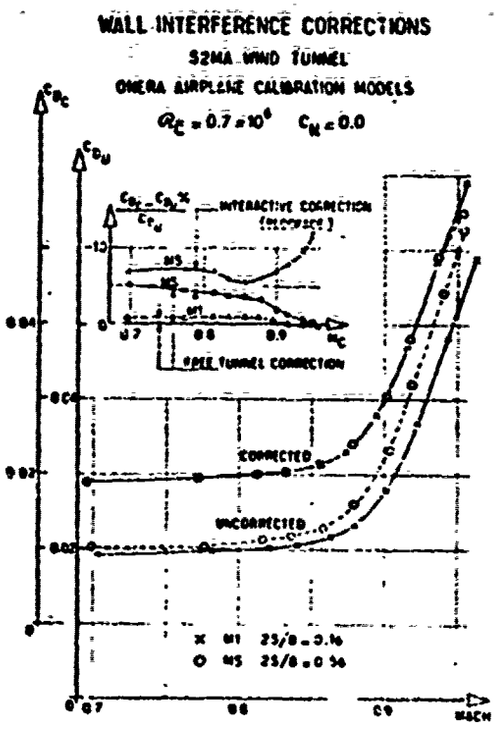

FIG. 21.

The importance of the two corrections for drag has already been emphasized on the basis of comparative tests made on models of C5A [14] and YF16 [15] aircraft in NASA Ames 11T, Calspan 8T and AEDC 16T wind tunnels.

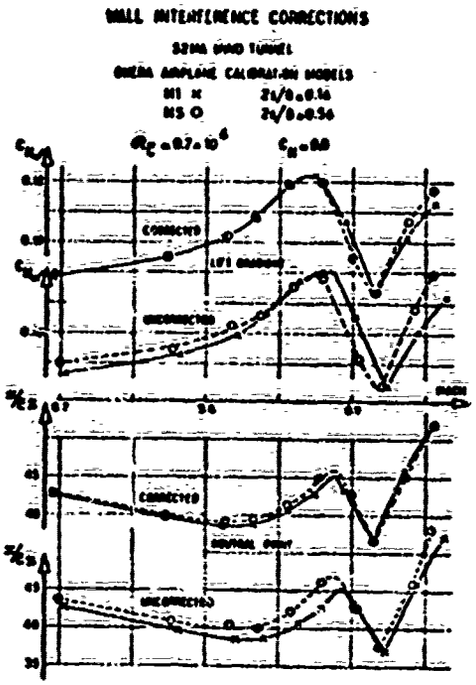

FIG. 22.

2.7. Effect of Roughness

The procedure of using roughness to trigger transition is often adopted to increase the reliability of wind tunnel tests and, in particular, to weaken the sensitivity of the pitching moment at zero lift to the Reynolds number and the effects of flow fluctuations by linearizing the stability curves. Thus, it seems natural to conduct the comparative tests in the triggered transition in order to reduce the developments with the Reynolds number and, consequently, the deviations between the results obtained from different wind tunnels. Tests of this type were made by AEDC and NASA Ames on two ONERA calibration models, M3 and M5, in reference to identical tests in natural transition at Mach 0.84 and different Reynolds numbers.

The comparison of the pressure distributions on the cross section of the wing tip, given at a local Reynolds number of 1.7 million (Fig. 23), shows the very significant effect of roughness: it provokes a 24% advance of the shock and causes the boundary layer at the trailing edge to thicken. In the natural transition, the position of transition is on the upper wing surface at the point where the shocks provoke the transition.

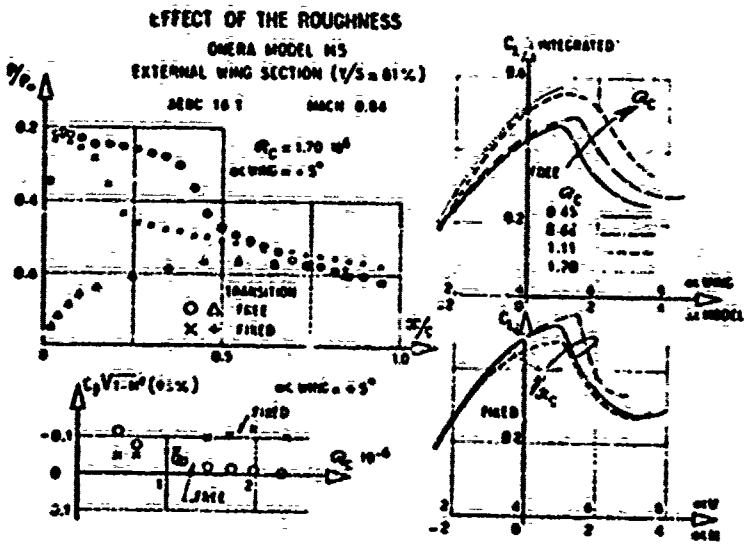

FIG. 23.

The developments in the pressure coefficients of the trailing edge and lift integrated with respect to the Reynolds number are reversed from free transition to triggered: at the highest Reynolds number, roughness excites premature stalling at a negative angle of attack of the model.

As for the overall characteristics of the model (Fig. 24), the roughness produces a clear increase in drag, a decrease in the lift-drag ratio of approximately 20% and an increase in the lift gradient of the same order. The focus remains in the same position. The developments accompanying the Reynolds number are uniquely changed with respect to drag and lift-drag ratio: the

roughnesses increase the drag variations by displacing the transition zones toward low numbers from 0.5 to 1.5 million. On the other hand, the lift-drag ratio changes the least.

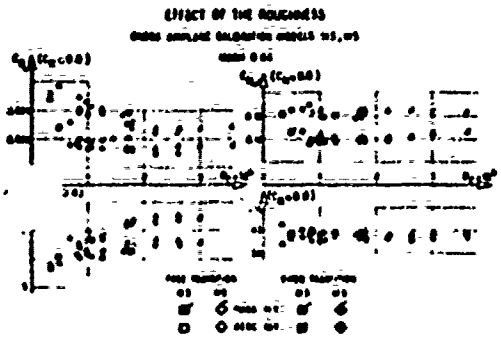

Fig. 24.

From the viewpoint of the comparison of the results, it does not appear that the roughness has reduced the divergences between the results coming from two different models and wind tunnels. On the contrary, the deviations in drag, the lift-drag ratio and lift increased in the triggered transition.

Thus, tests in the triggered transition on models with profiles having a high velocity gradient can be criticized for the adverse effects they can generate.

The use of roughness does not improve the deviations in the comparative measurements. Roughness characteristics (placement and dimensions) depend on the flows inherent in each wind tunnel and the local velocity gradients of each type of profile and their angle of attack.

2.8. Flow Around Mach 1

Comparisons were made of the distribution of pressure and drag of a rotating body C5 which had the same law of areas as

calibration model M5 among the AEDC 16T, NASA Ames 11T and S2 Modane 6T wind tunnels between Mach 0.7 and 1.0. The drag coefficients agree well (Fig. 25) between Mach 0.85 and 1.00, which was rather surprising in view of the discrepancies noted for airplane model M5 (Figures 11, 18 and 20), which were 9.8% at Mach 0.84 for the three wind tunnels compared.

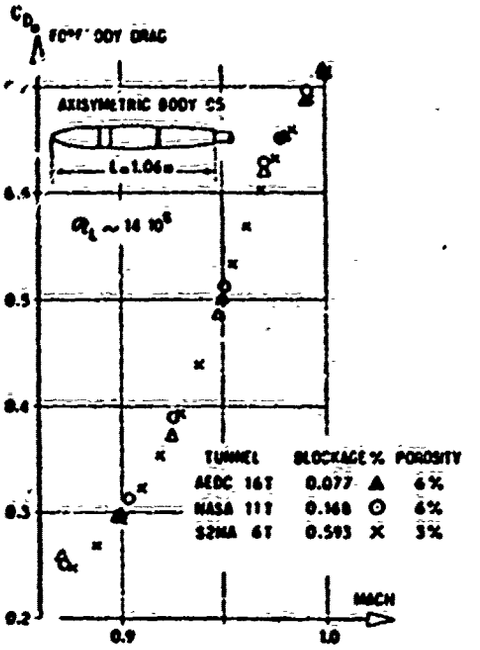

Fig. 25.

The first reason for the excellent agreement of the results from rotating body C5 is no doubt the absence of an airfoil. The wing on model M5 produced discrepancies caused by the position of transition and breakaway on the trailing edge along the span, resulting in a change in the friction drag. On the other hand, the flow is turbulent from the nose on for the rotating body, like for an airplane fuselage model.

Another reason for the discrepancies in the airplane model is a result of the positions of the shock waves and the breakaway preceding them. These discrepancies do not result in discrepancies

in drag on the rotating body, for the pressure deviations at the end of the nose section (Fig. 26) are compensated for by those existing at the base constraint due to balances brought about by the local gradients of the generators which lead to the drag coefficient.

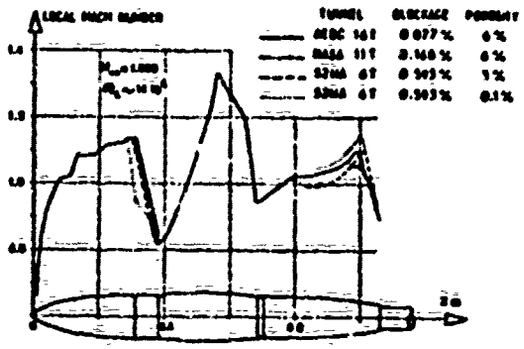

Fig. 26.

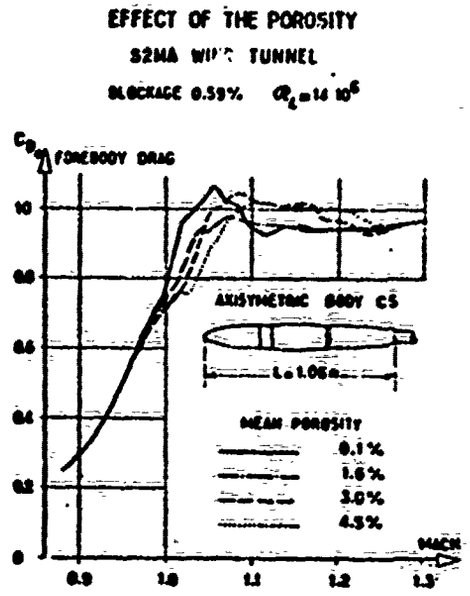

Fig. 27.

Tests were made in the S2 Modane wind tunnel in the upper transonic at various wall permeabilities. The effect of wall permeability on drag shows up above Mach 0.95 (Fig. 27): an increase in permeability reduces drag between Mach 0.95 and 1.07, then increases it between 1.07 and 1.20.

Actually, the increase in permeability always results in a decrease in pressure, but only on the nose section below Mach 1.07 and, most of all, in the breakaway zone behind the prime pair between Mach 1.07 and 1.12. These effects combine so that the variation in the drag component reverses at Mach 1.07. In this Mach range and up to Mach 1.22, the waves emitted by the model interact with it after being reflected off the walls. Shadow

photographs show reflected waves which are all the more intense and displaced forward as permeability increases. The largest number of these waves can be seen at Mach 1.07, where the pressure deviations are the greatest, although the drags happen to be identical. Thus, it seems that as the Mach number increases from 0.9 to 1.07, it is very important to progressively reduce wall permeability in order to obtain the most correct results.

CONCLUSIONS

The most important lessons which can be learned from comparing transonic wind tunnels are the following:

- In two-dimensional flow, it is indispensable to eliminate the effects of the boundary layer of the lateral walls. Drag determined by combing wakes is affected very little by wall effects. It is identical for the same model in the ONERA S3MA and the NAE 5T wind tunnels. The other coefficients require major corrections which can be correctly regrouped after making corrections for the wind tunnels in question, in spite of the difficulty of determining the coefficient characterizing perforated test sections. These coefficients make it possible to see the effect of the Reynolds number up to $40 \cdot 10^6$.

- In three-dimensional flow, the comparison of various wind tunnels using the ONERA calibration models of a representative transport aircraft shows that major discrepancies occur in the transonic range (Mach 0.7 to 0.96). These deviations are reduced to one-third of their value by considering only models which are relatively small ($s/b \leq 0.2$). These deviations can be reduced by applying corrections which account for the precise calibration of the test sections to the results. Large models require additional corrections to account for the interference created by the test section walls. An example shows that the agreement between the results obtained on two models can be compatible with the

scattering of measurements after all the corrections are made. Only after these corrections are applied can the results obtained in different wind tunnels be classified as a function of the flow fluctuation levels.

ACKNOWLEDGEMENTS

ONERA wishes to emphasize the cooperation of the organizations which contributed to the comparative studies and to thank those responsible for the tests in particular, in chronological order:

M. Menard - Saint-Cyr Aerotechnological Institute
W. Lorenz-Meyer - AVA Göttingen
S. E. Gudmundson - FFA Stockholm
F. W. Steinle, Jr. - NASA Ames
T. W. Binion - AEDC Tullahoma
L. N. Onman - NAE Ottawa

BIBLIOGRAPHY

[1] M. BAZIN
Dispositif d'essais de profils en courant plan dans la soufflerie S3 de Modane-Avrieux
NT ONERA n° 203 - 1972

[2] L.H. CHIANG
The NAE High Reynolds number 15 in x 60 in two dimensional test facility
LTR - HA - 4 - NAE - Avril 1976

[3] M. HOSNY
Higher order theory of two-dimensional subsonic wall interference in a perforated wall wind tunnel
NRC Aero Report LR 553 Octobre 1971

[4] M. HOSNY
Wall interference on two-dimensional supercritical airfoils using wall pressure measurements to determine the porosity factors for tunnel floor and ceiling
NRC - Aero Report LR 575 Feb.1974

[5] P.BAZIN - R.BERNARD DUBOIS - J.CHEVALIER
Critique des techniques d'essais de profils transoniques
Aéronautique et Astronautique n°31 et 32 (1971)

[6] A review of measurements on AGARD calibration models
AGARDOGRAPH 64 - Nov. 1961

[7] P. POISSON-QUINTON
Information in a round-table discussion about ONERA calibration models and test results.
AGARD CP n° 83 (pp B-7 - B-12)

[8] X.VAUCHERET
Comparaison de souffleries transsoniques à l'aide de maquettes étalons ONERA
LAMS PAPER n°77 - Avril 1972

[9] S.E. GUDMUNDSON
Comparative tests with ONERA Airplane calibration models in FFA transonic wind-tunnels.
EUROMECH 40 - Colloquium transonic Aerodynamics
Sept. 1973

[10] M.S. DOUGHERTY Jr - P.W. STEINLE Jr
Transition Reynolds number comparison in several major transonic tunnels
AIAA Paper n° 74-627 July 1974

[11] J.CH VAYSSAIRE
Survey of methods for correcting wall constraints in transonic wind tunnels
AGARD Report n° 601 - Nov. 1972

[12] M. MENDOLA C.P. LO
Boundary interference at subsonic speeds in wind tunnels with ventilated walls
AEDC TR 69-47 May 1969

[13] X. VAUCHERET - J.CH VAYSSAIRE
Corrections de parois en écoulement tridimensionnel transsonique dans des veines à parois perforées
Symposium AGARD/FDP - Londres Oct. 1975

[14] S.L. TREON - P.W. STEINLE and Alii
Further correlation of data from investigations of a high subsonic speed transport aircraft model in three major transonic wind tunnels
AIAA Paper n° 71-291 March 1971

[15] J.M. BUCHER - J.B. PEEP
Selected results from the YF 16 wind tunnel test program
AIAA Paper n° 74-619 July 1974